Supporting Information

Compartmentalization of Alkaline Earth Metals in Salen-type Cu- and Ni-Complexes in Solution and in the Solid State

Alba Finelli [†], Nelly Hérault [†], Aurélien Crochet [‡], Katharina M. Fromm [*,†]

[†] Department of Chemistry, University of Fribourg, Ch. du Musée 9, 1700 Fribourg, Switzerland
[‡] FriMat, Department of Chemistry, University of Fribourg, Ch. du Musée 9, 1700 Fribourg, Switzerland.

Table of Contents

General

All experiments were performed in air and at RT. Ligand **H_2L** was prepared according to the procedure reported by Avecilla et *al.* previously. All chemicals were commercial products of reagent grade and were used without further purification. ^{1}H and ^{13}C measurements were carried out for the Ni-compounds with a Bruker 400 MHz spectrometer at ambient temperature, and chemical shifts are given in ppm with respect to the residual solvent peak. Mass spectra (ESI-TOF, positive mode) were recorded with a Bruker esquire HCT spectrometer with a DMF/ACN mixture as solvent. The UV/Vis spectra were recorded with a Perkin-Elmer Lambda 40 spectrometer. The crystallographic data of single crystals were collected with Mo-K_α radiation (λ = 0.71073 Å). Powder X-ray spectra were collected on a Nonius Enraf FR 590 X-ray generator with mounted Stoe StadiP using Cu Kalpha1 radiation (1.5406 A˚).

All measurements were performed at 200 K, or 250 K for the compounds **5** and **8**, with Stoe IPDS-II or IPDS-II T diffractometers equipped with Oxford Cryosystem open-flow cryostats. Single crystals were picked under the microscope, and placed in inert oil. All crystals were mounted on loops and all geometric and intensity data were taken from one single crystal. The absorption corrections were partially integrated in the data reduction procedure. The structures were solved and refined using full-matrix least-squares on F^2 with the SHELX-2014 package. All atoms (except hydrogen atoms) were refined anisotropically. Hydrogen atoms were refined where possible, and otherwise added using the riding model position parameters.

NMR Titration of metallohost LNi

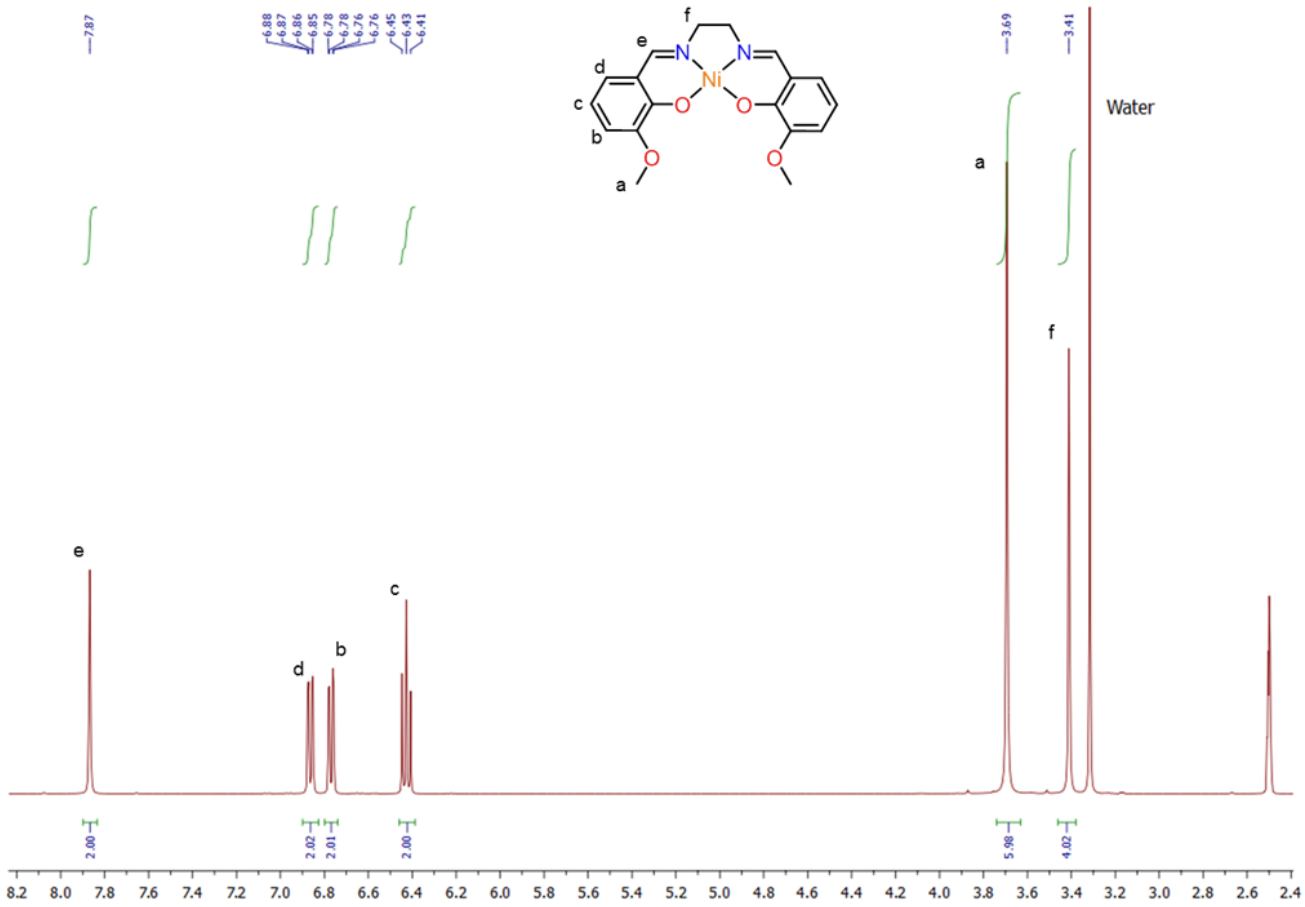

Figure S1: ^{1}H NMR spectrum of LNi (400 MHz, DMSO-d_6, 0.02 M).

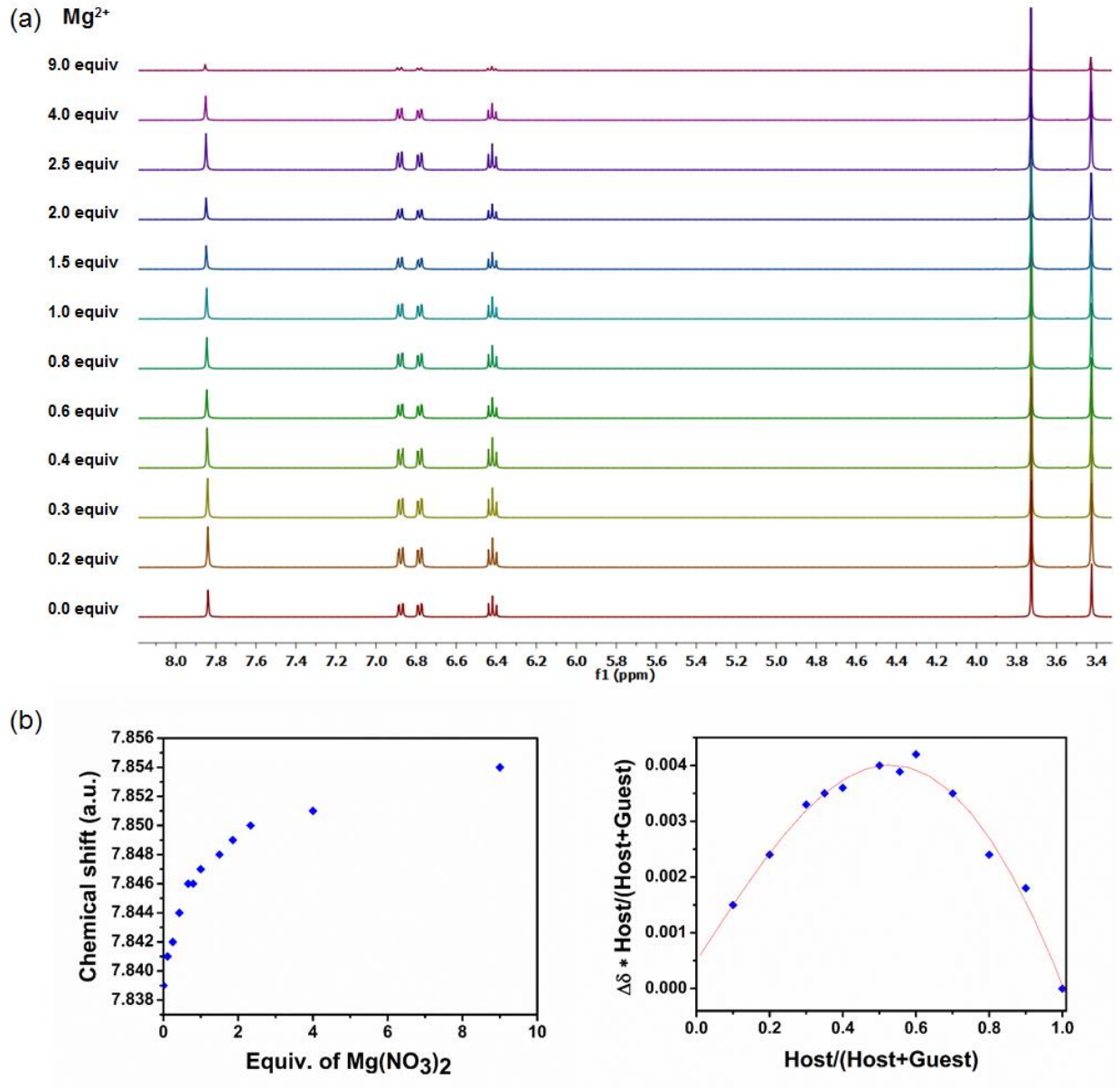

Figure S2: a)^{1}H NMR spectral changes of the metallohost LNi (400 MHz, DMSO-d_6, 0.04 M) upon the addition of $Mg(NO_3)_2$ in deuterated DMSO b) the corresponding isotherm curve and the Job plot.

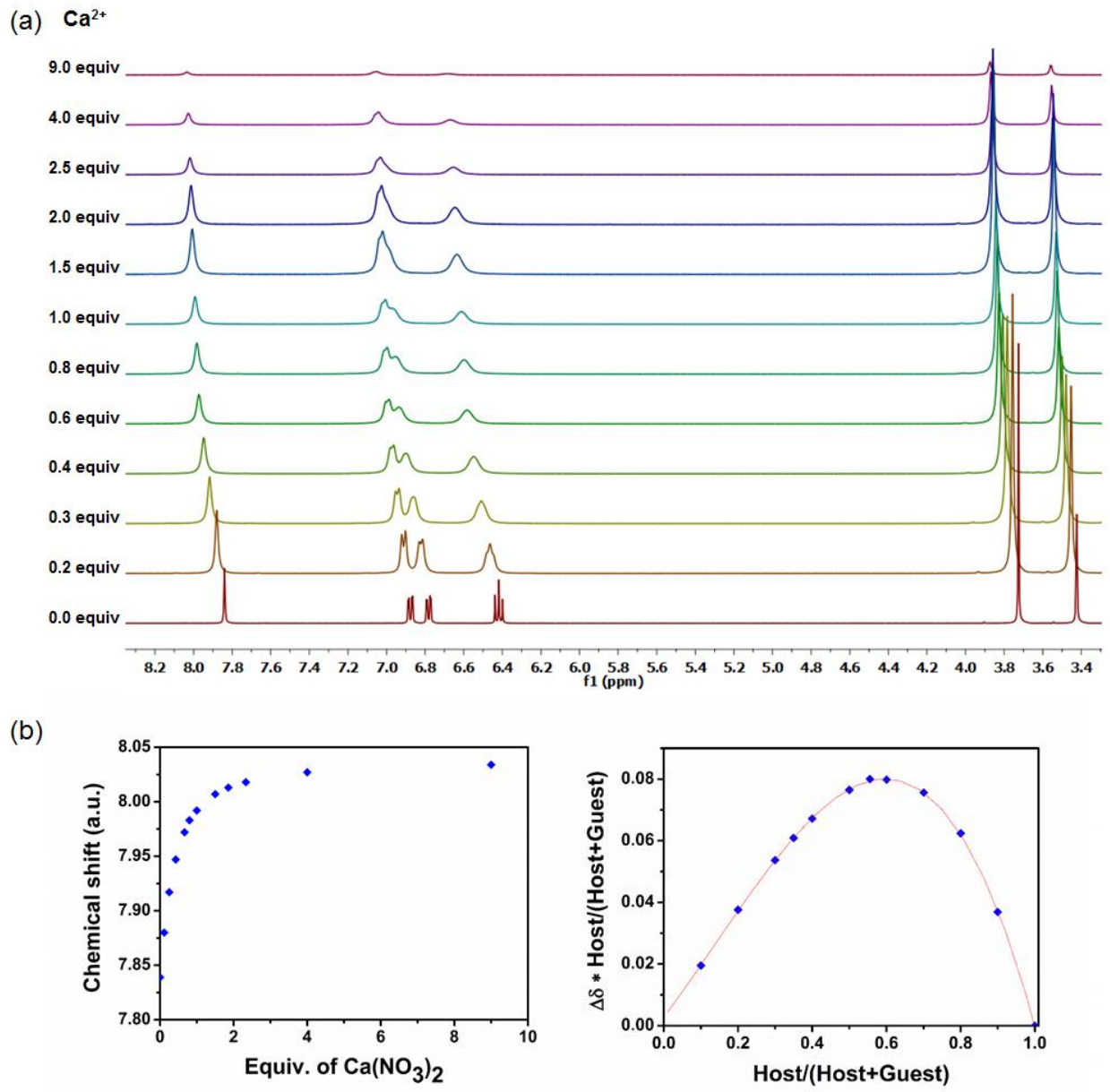

Figure S3: a)^{1}H NMR spectral changes of the metallohost LNi (400 MHz, DMSO-d_6, 0.04 M) upon the addition of $Ca(NO_3)_2$ in deuterated DMSO b) the corresponding isotherm curve and the Job plot.

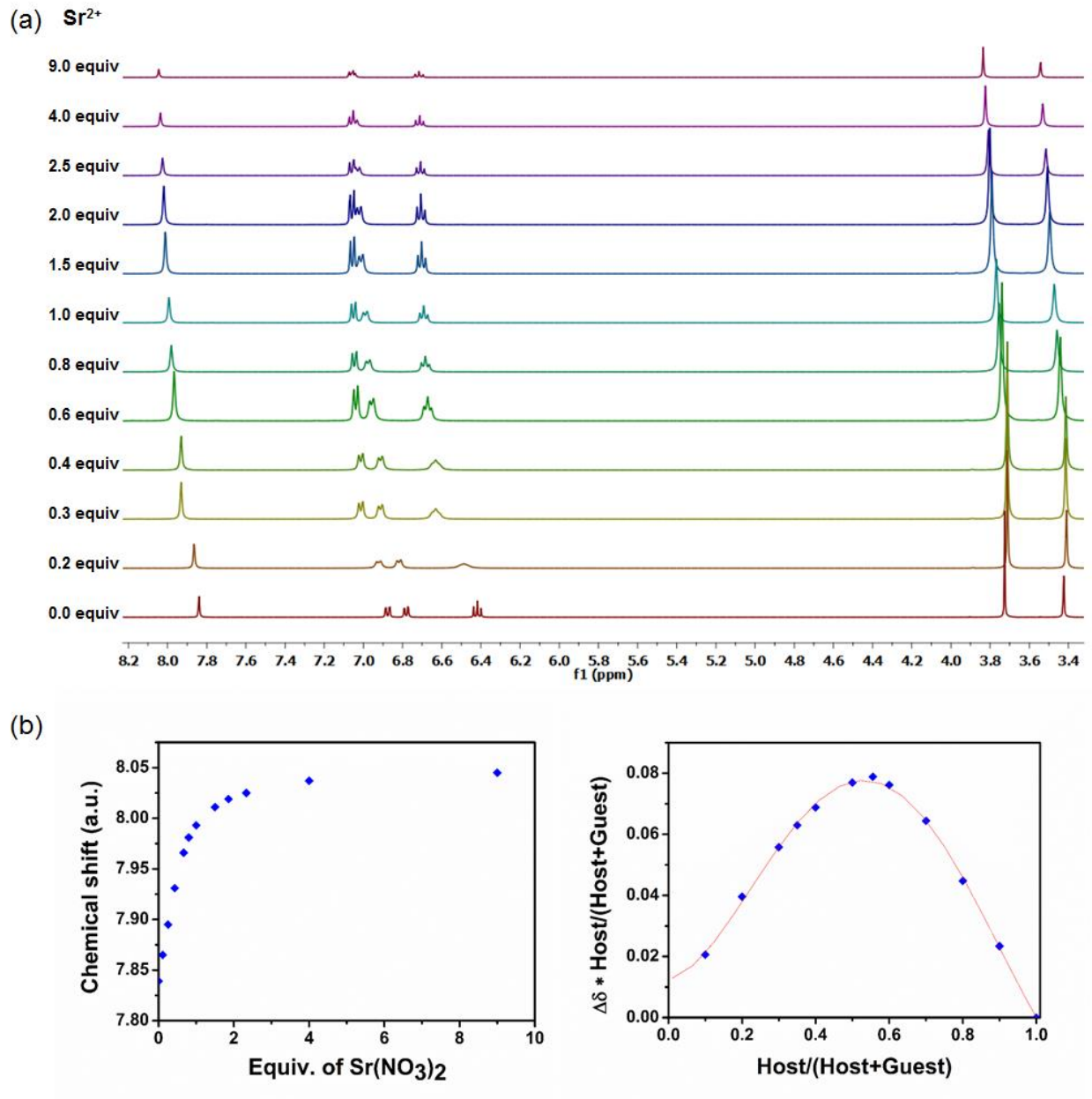

Figure S4: a)^{1}H NMR spectral changes of the metallohost LNi (400 MHz, DMSO-d_6, 0.04 M) upon the addition of $Sr(NO_3)_2$ in deuterated DMSO b) the corresponding isotherm curve and the Job plot.

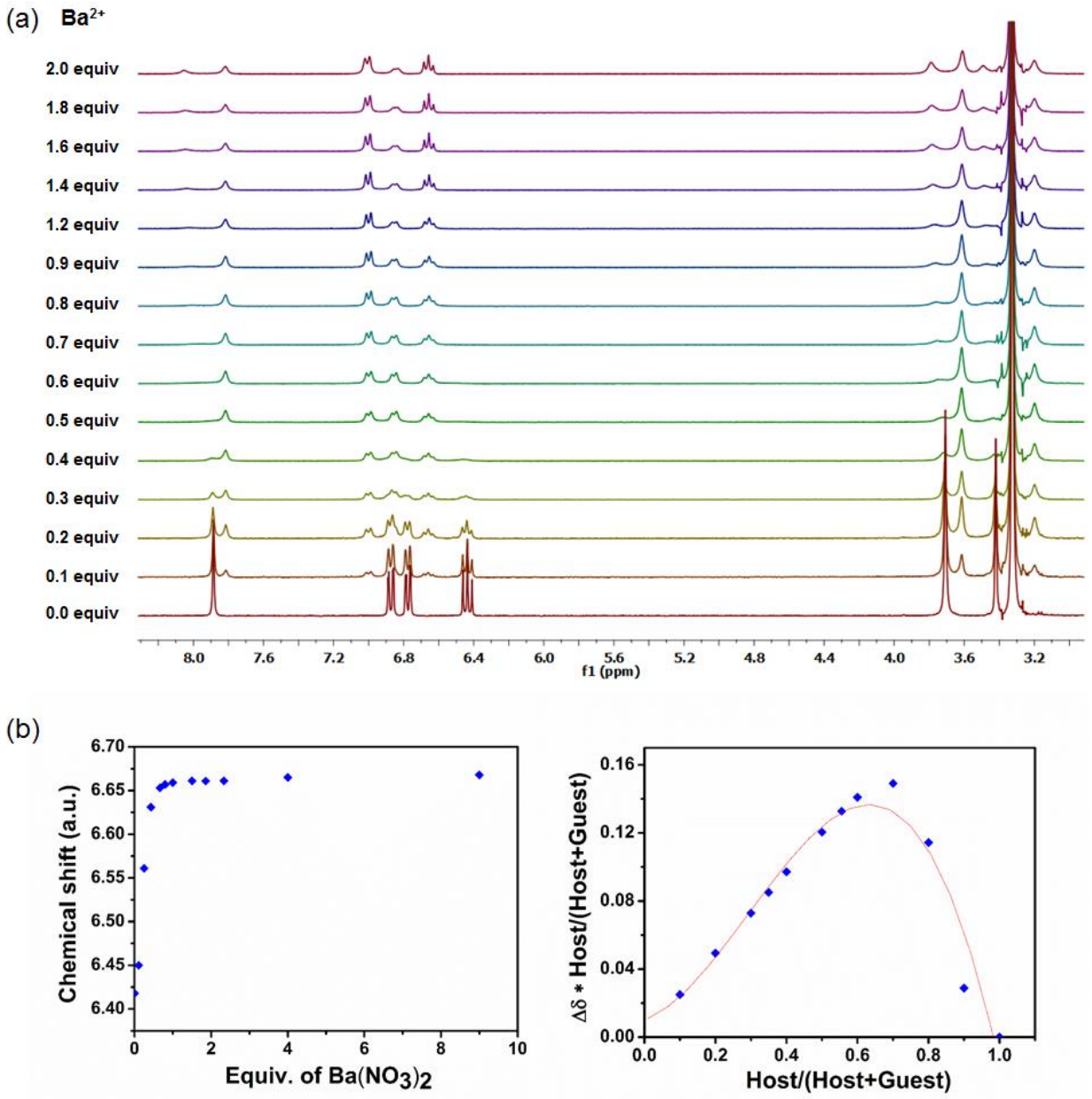

Figure S5: a)^{1}H NMR spectral changes of the metallohost LNi (400 MHz, DMSO-d_6, 0.04 M) upon the addition of $Ba(NO_3)_2$ in deuterated DMSO b) the corresponding isotherm curve and the Job plot.

UV-Vis Titration of the metallohost LCu

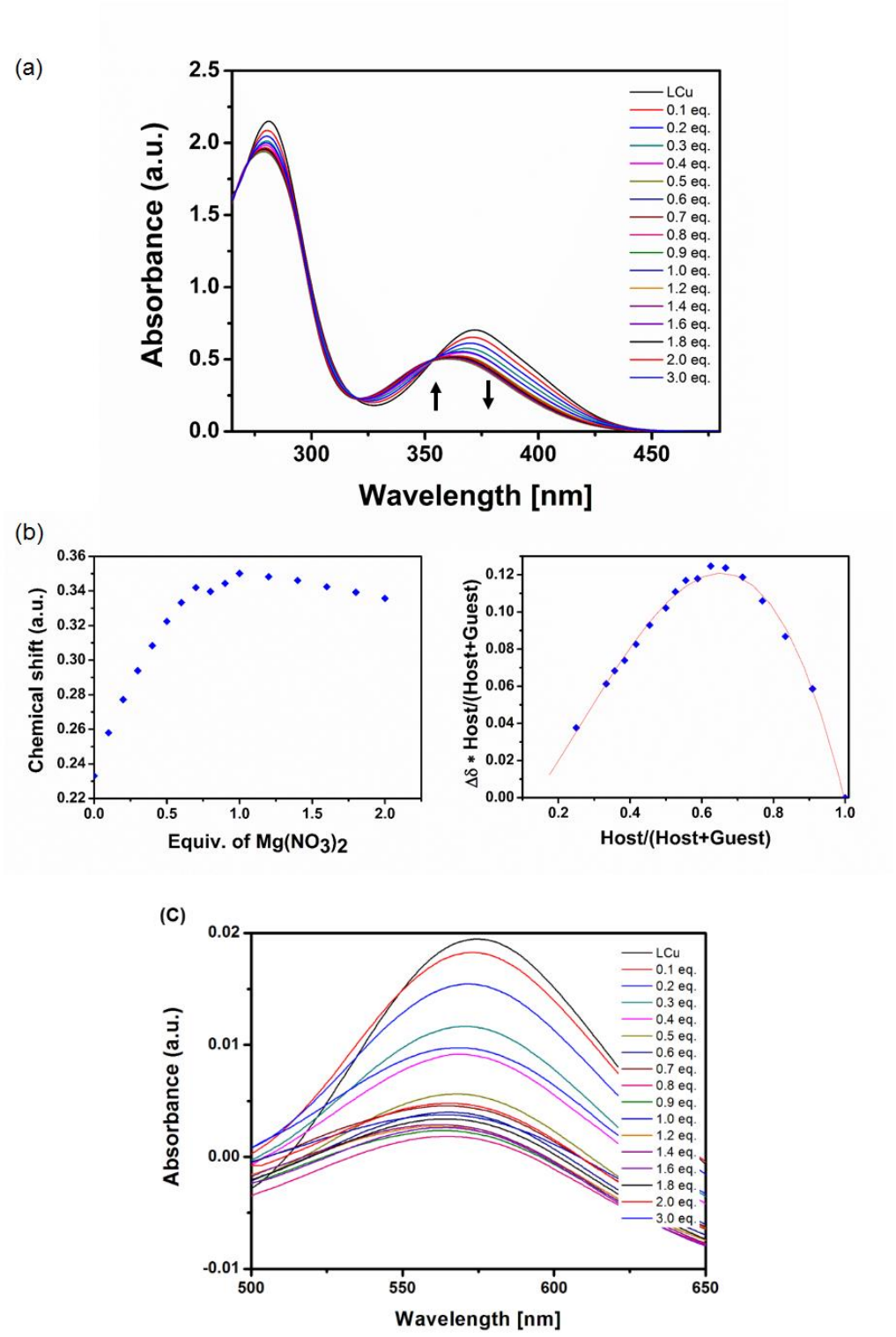

Figure S6: a) UV-Vis spectral changes of the metallohost LCu (0.1 mM) in ACN upon the addition of a solution of $Mg(NO_3)_2$ in DMSO, b) the corresponding isotherm curve and the Job plot, c) zoom of the spectrum between 500 and 650 nm.

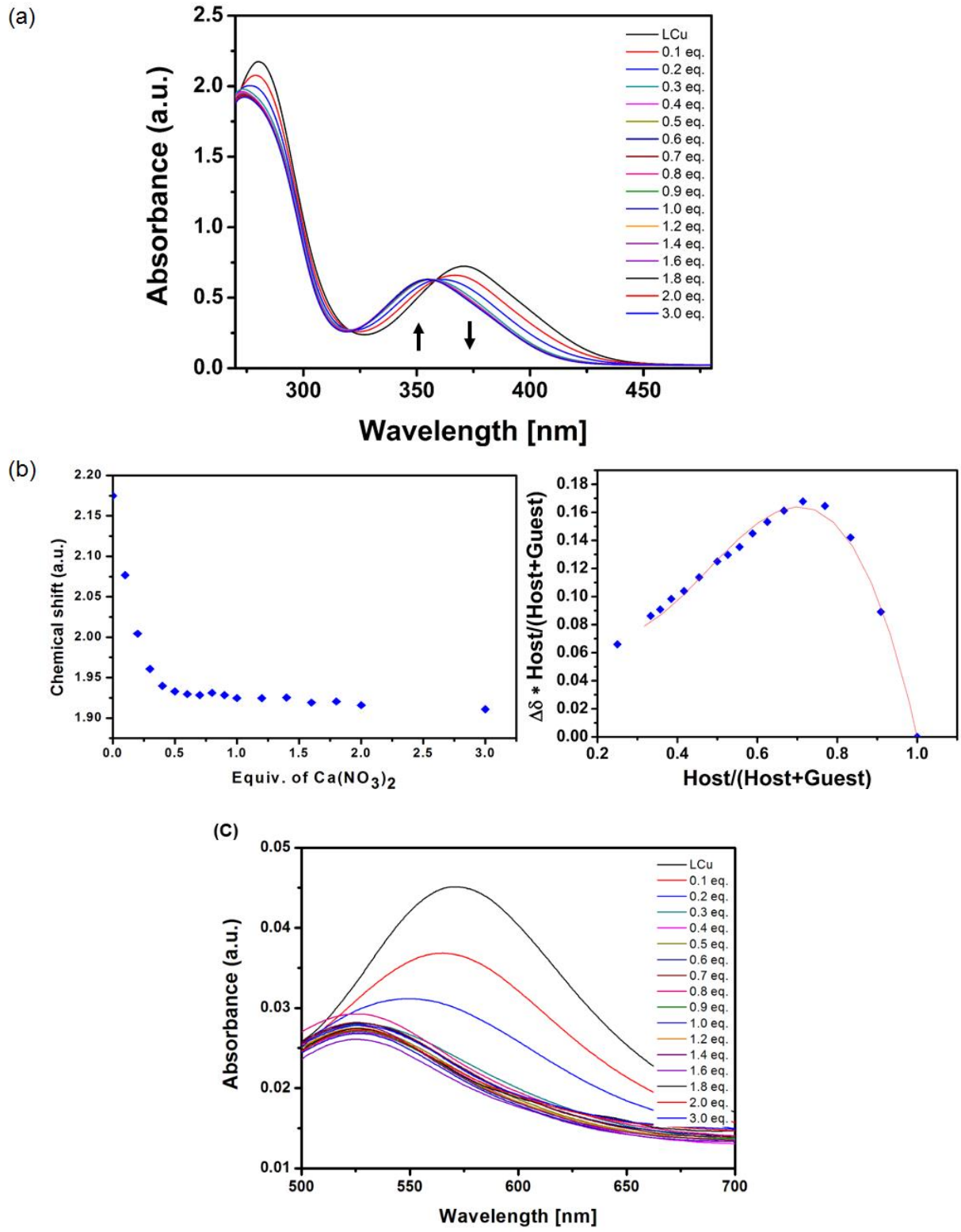

Figure S7: a) UV-Vis spectral changes of the metallohost LCu (0.1 mM) in ACN upon the addition of a solution of $Ca(NO_3)_2$ in DMSO, b) the corresponding isotherm curve and the Job plot, c) zoom of the spectrum between 500 and 650 nm.

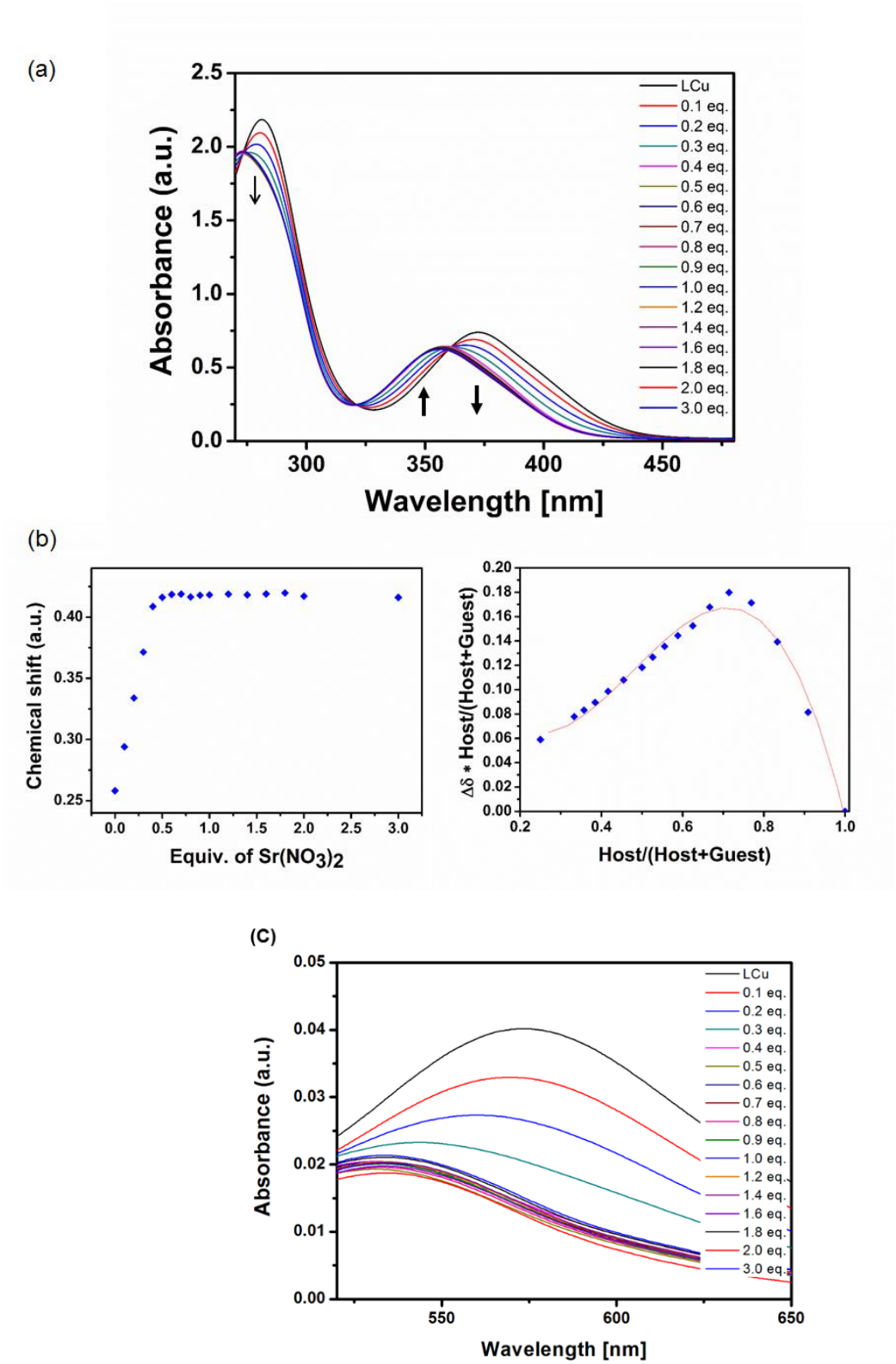

Figure S8: a) UV-Vis spectral changes of the metallohost LCu (0.1 mM) in ACN upon the addition of a solution of $Sr(NO_3)_2$ in DMSO, b) the corresponding isotherm curve and the Job plot, c) zoom of the spectrum between 500 and 650 nm.

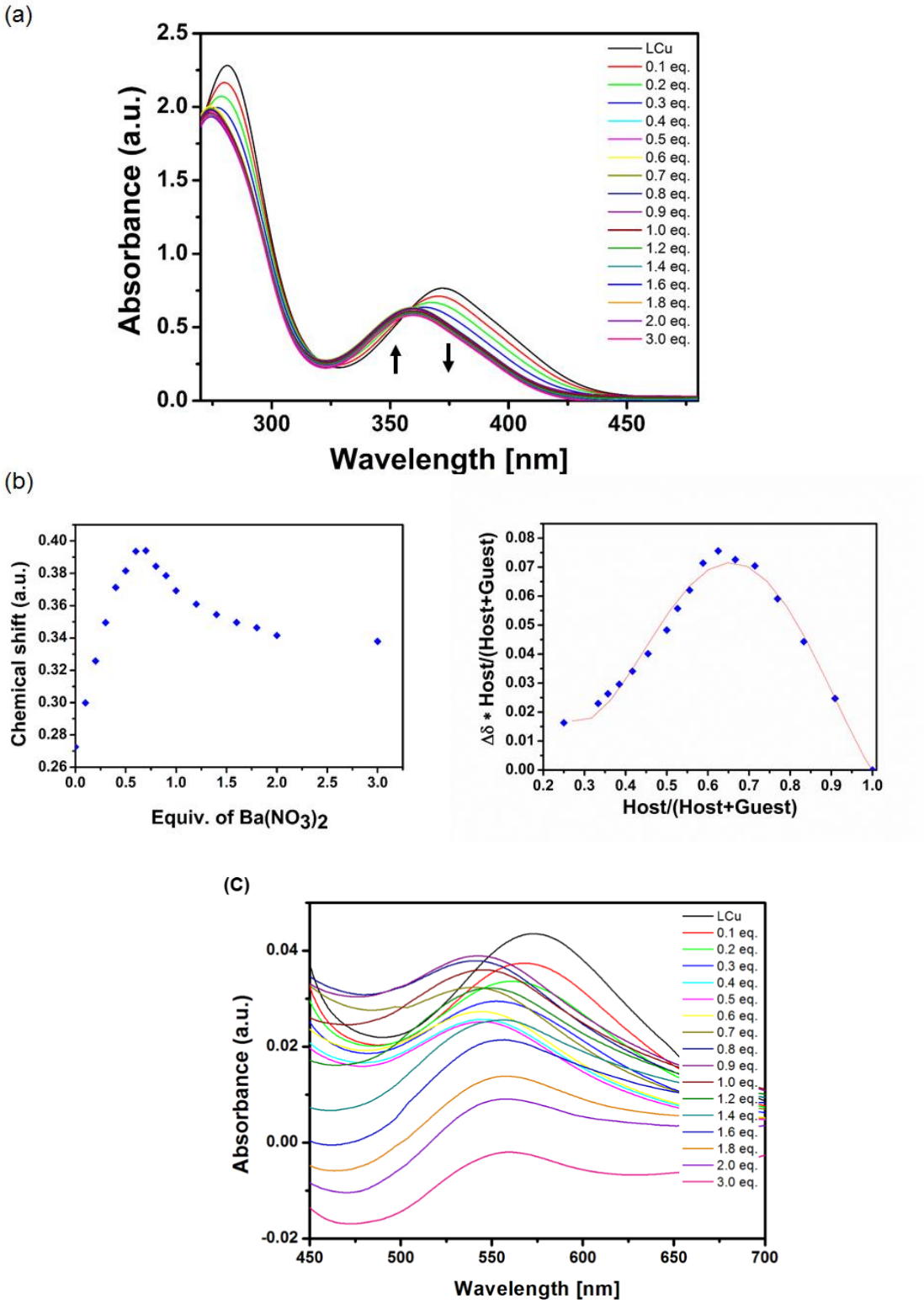

Figure S9: a) UV-Vis spectral changes of the metallohost LCu (0.1 mM) in ACN upon the addition of a solution of $Ba(NO_3)_2$ in DMSO, b) the corresponding isotherm curve and the Job plot, c) zoom of the spectrum between 450 and 650 nm.

Powder X-Ray

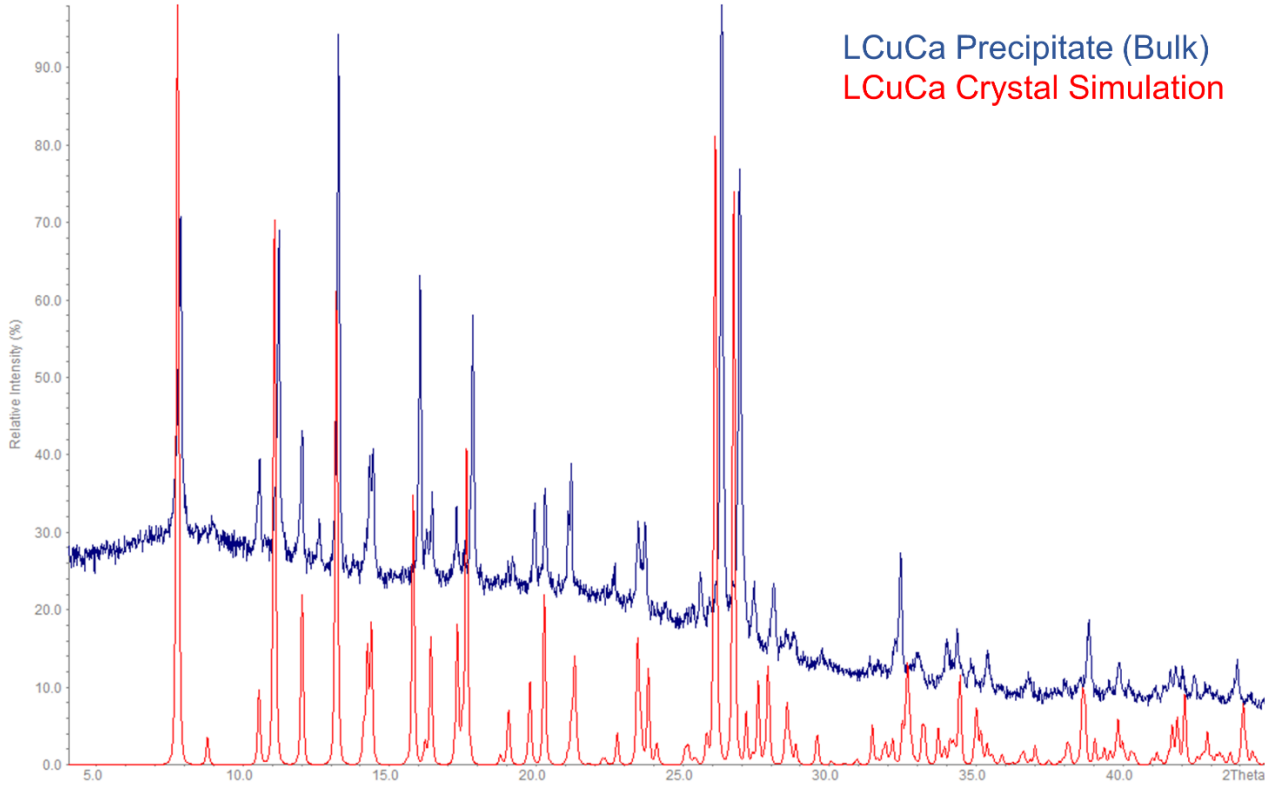

Figure S10: XPRD diffractogram of the LCuCa (2) precipitate compared with the crystal structure simulation 2.

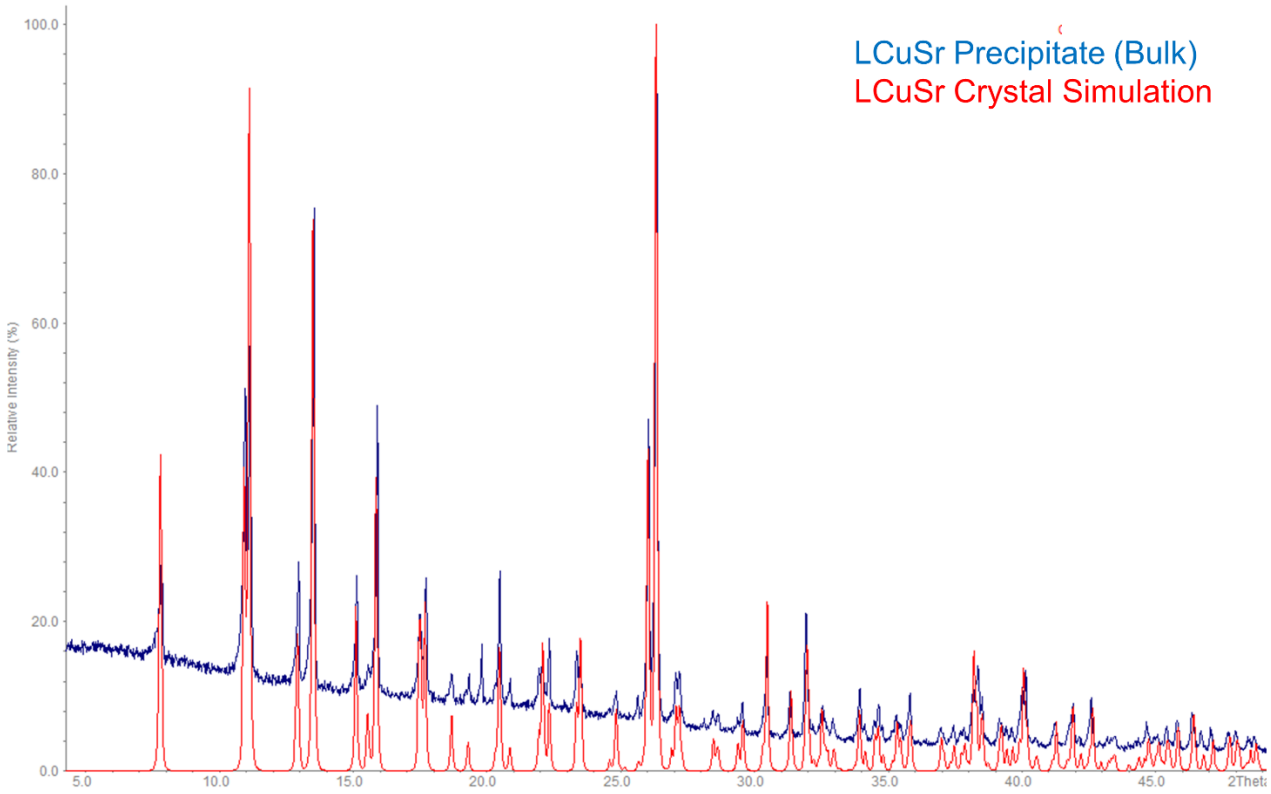

Figure S11: XPRD diffractogram of the LCuSr (3) precipitate compared with the crystal structure simulation 3.

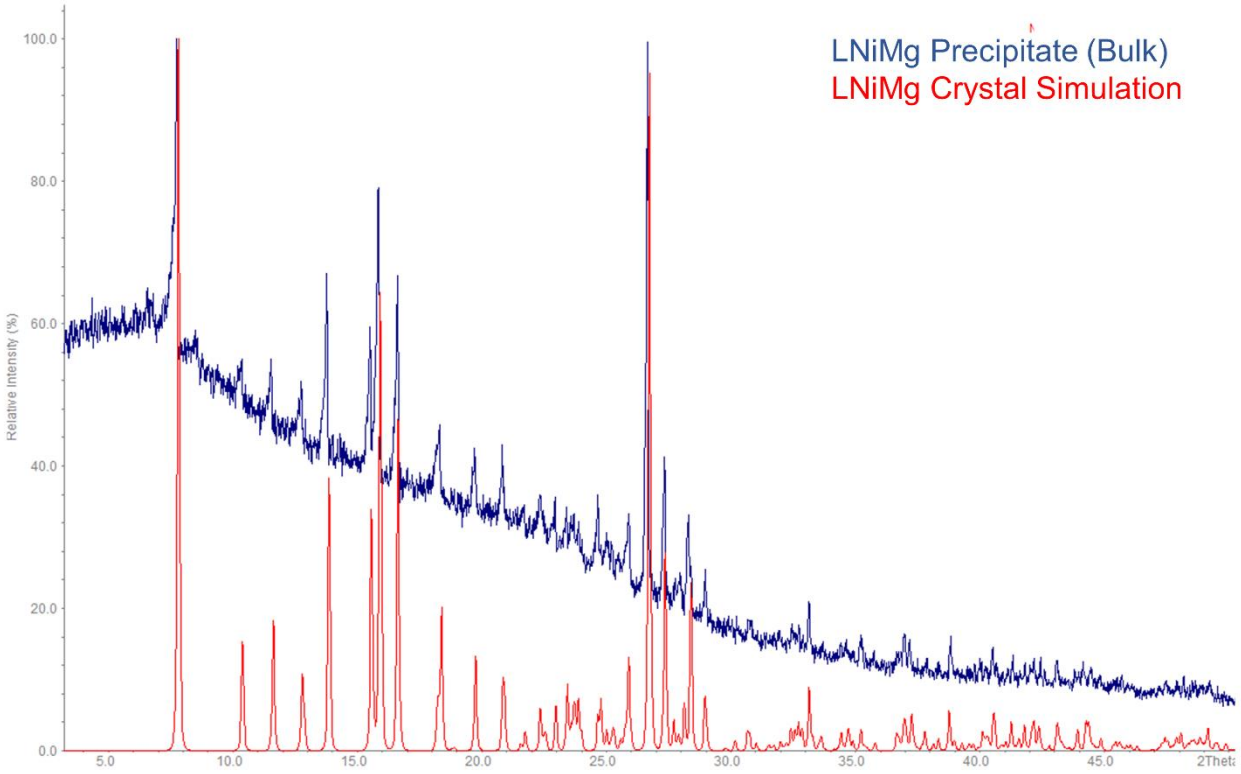

Figure S12: XPRD diffractogram of the LCuBa (4) precipitate compared with the crystal structure simulation 4.

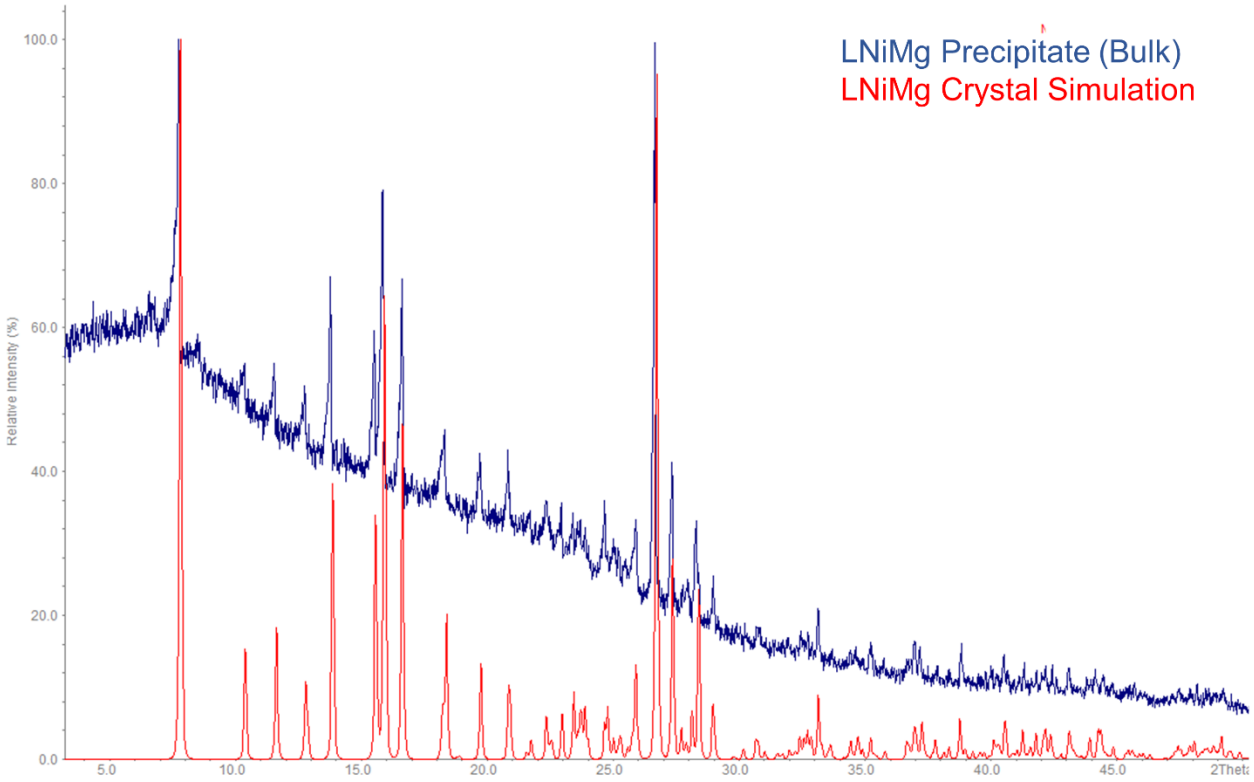

Figure S13: XPRD diffractogram of the LNiMg (5) precipitate compared with the crystal structure simulation 5.

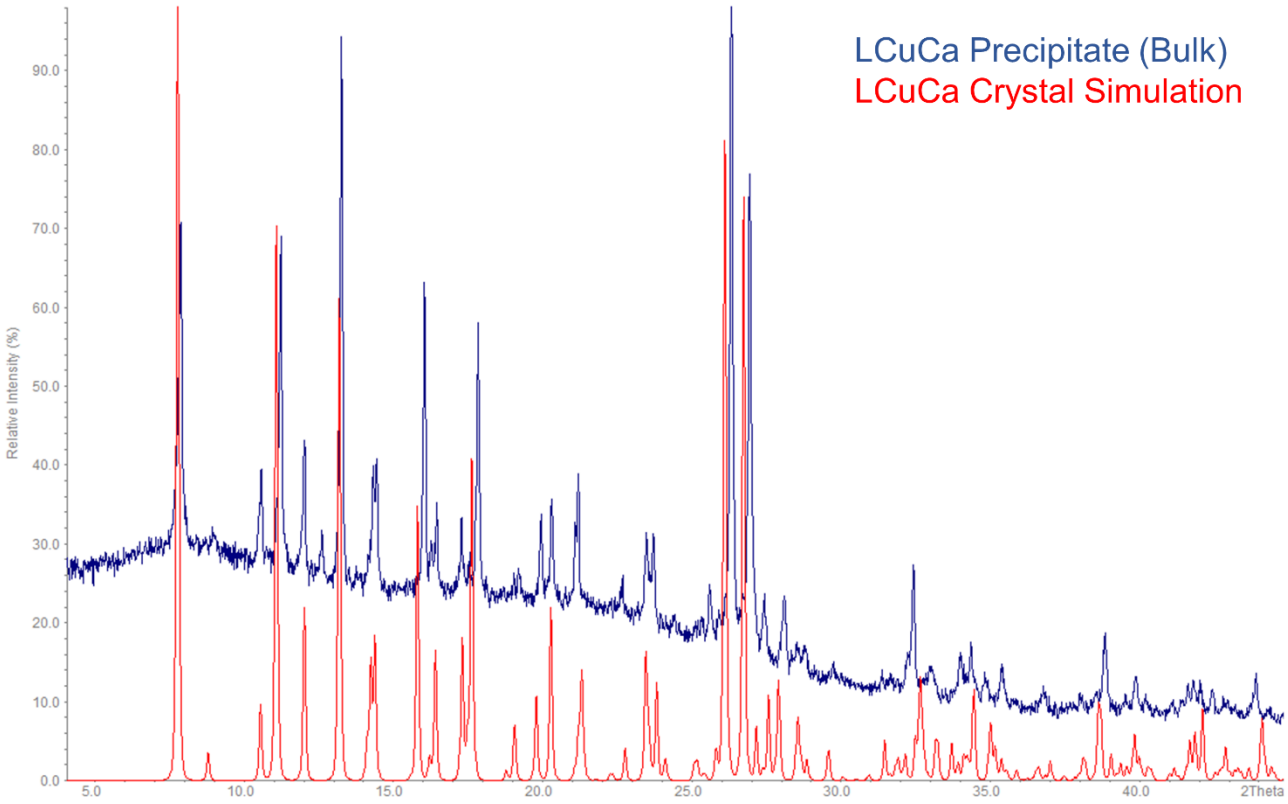

Figure S14: XPRD diffractogram of the LNiCa (6) precipitate compared with the crystal structure simulation 6.

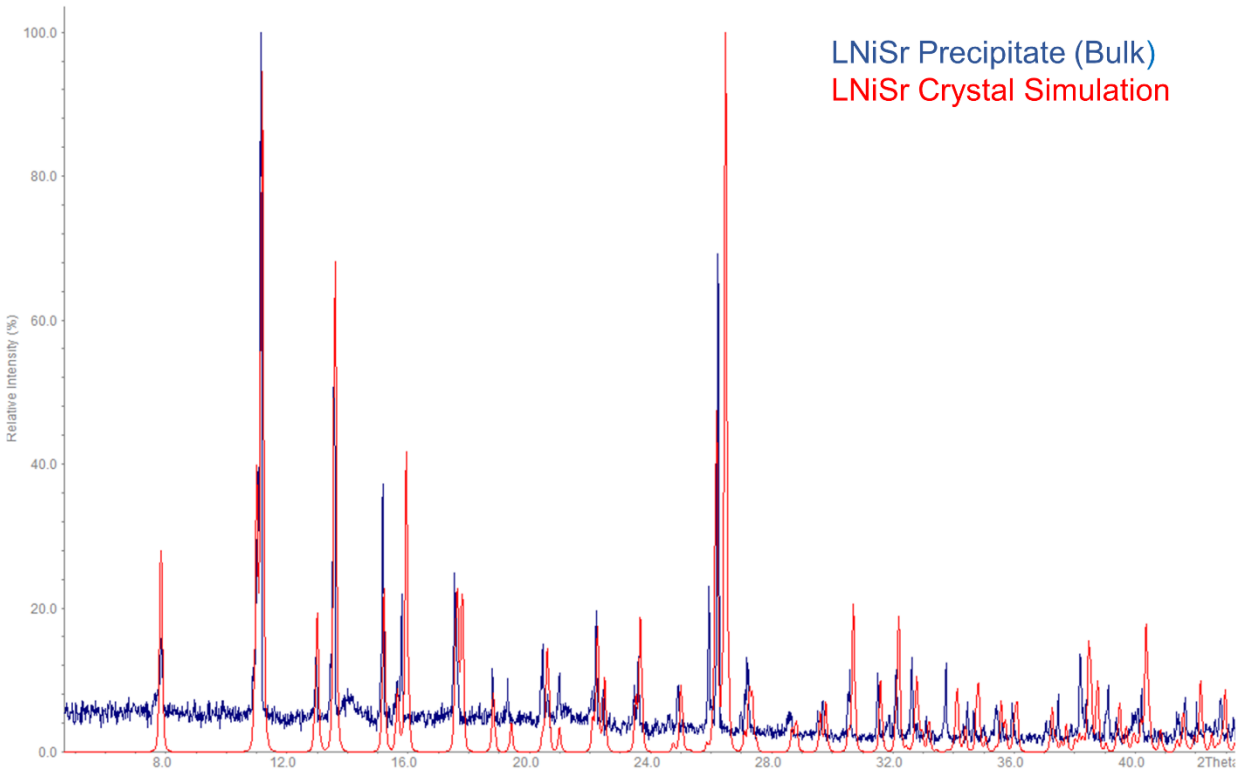

Figure S15: XPRD diffractogram of the LNiSr (7) precipitate compared with the crystal structure simulation 7.

Crystallography

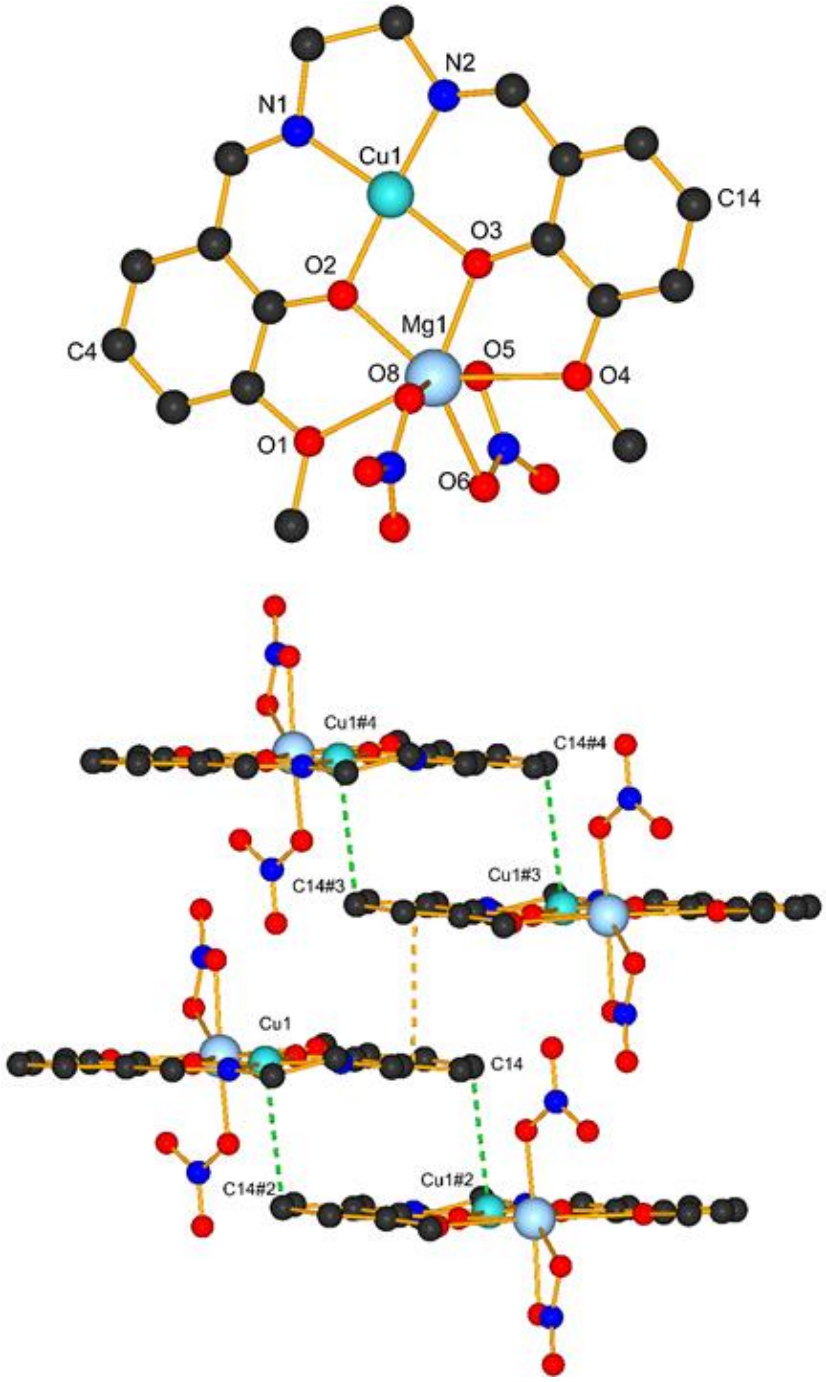

Figure S16: Crystal structure of **LCuMg** complex **1** (above, #2 (-x, 1-y, 1-z), #2(1-x, 1-y, 1-z), #3(1+x, y, z)), shows a π–π-system packing (orange dash bonds) and Cu(II)–C14 interaction (green dash bonds). H-atoms except for water are omitted for clarity.

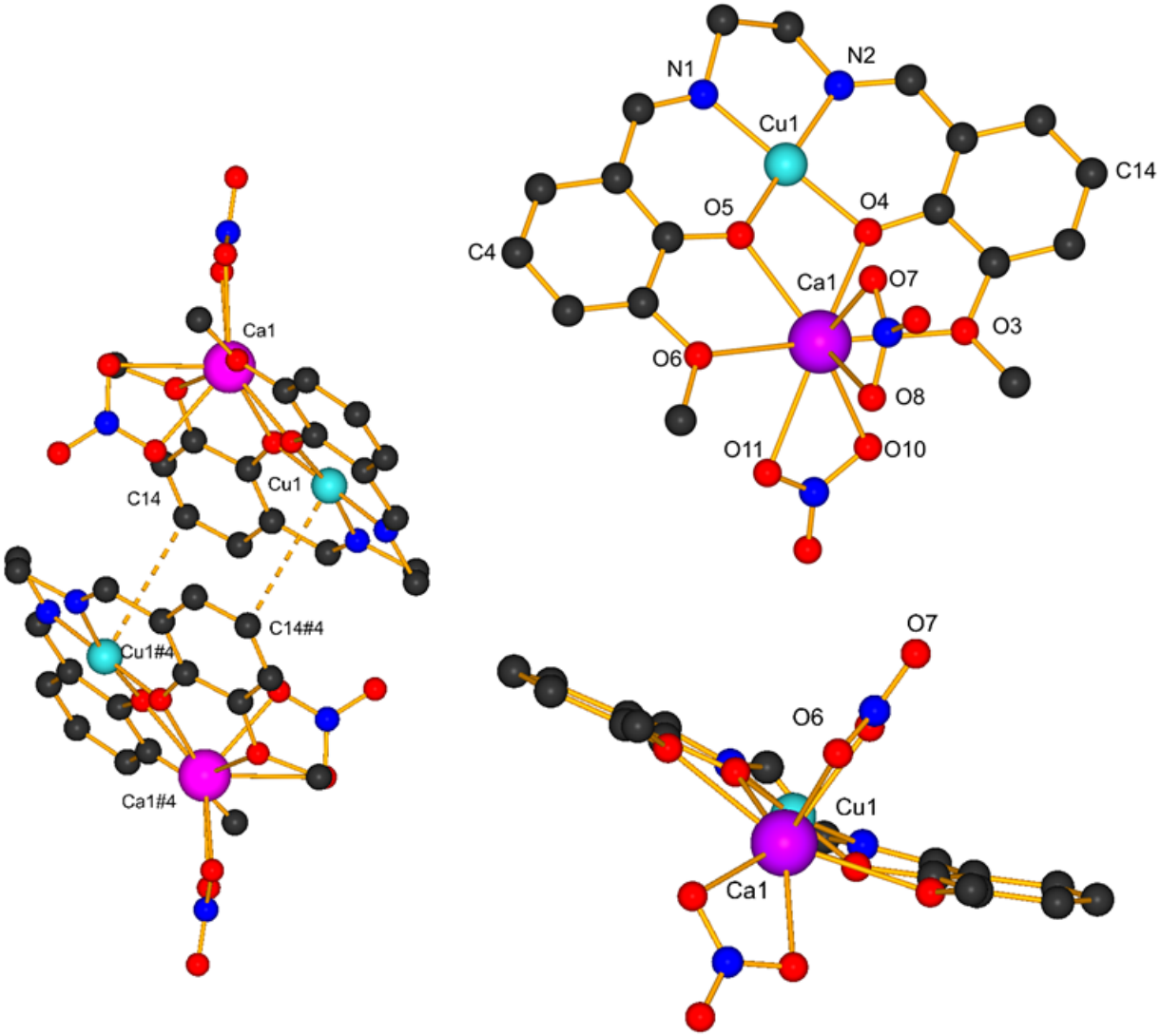

Figure S17 : Crystal structure of LCuCa complex 2 (#2 (1/2 -x, ½+y, ½-z), #3 (1/2 -x, -½+y, ½-z)), reveals a 1D coordination polymer expansion of the calcium ion via the neighbor O-atom O7 of a nitrate bridging ligand and Cu(II)–O6 weak bond (green dash bonds). H-atoms except for water are omitted for clarity.

.

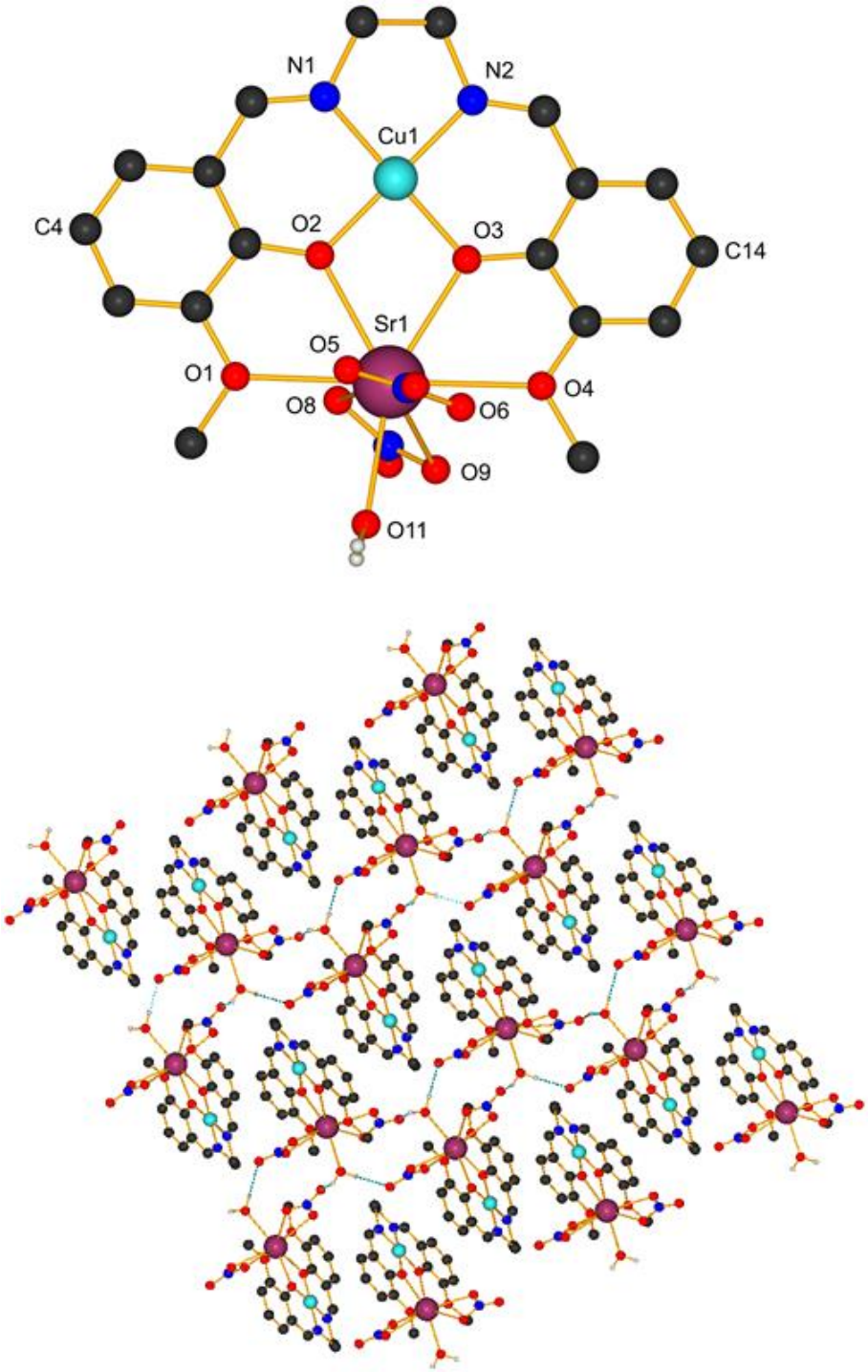

Figure S18: Crystal structure of LCuSr complex 3 (#2(x, -1+y, z), #3(½-x,- ½-y, ½+z), #4(½ -x, ½+y, ½+z),#4((½ -x, ½+y, -½+z)) presenting similar characteristics as compounds LNiCa (6) and LNiSr (7). Above, Cu(II)–C14 interaction (green dash bonds) and π–π-system packing interactions between two parallel neighbor unities (orange dash bonds). Below, presence of H-bonds creating different layers showed from the top and from the profile (blue dash bonds). All H-atoms except for water, are omitted for clarity.

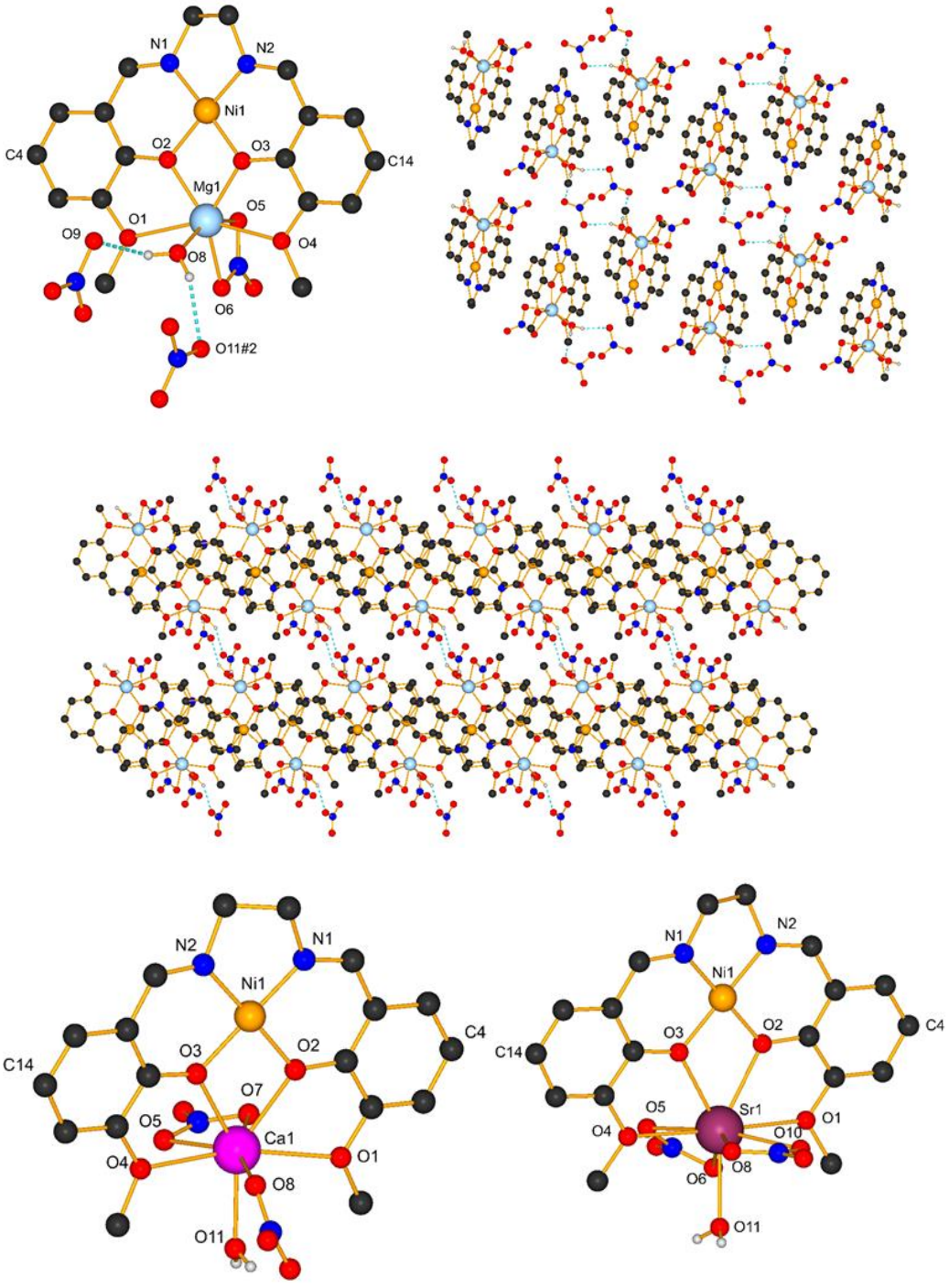

Figure S19: Crystal structure of LNiMg complex 5 presenting similar characteristics as compounds LNiCa (6) and LNiSr (7). They show Ni(II)–C4 interactions (green dash bonds) and π–π system packing interactions between two parallel neighbor unities (orange dash bonds). Below, presence of H-bonds creating different layers showed from the top, creating channels along *a*-axis occupied by two nitrate ions (blue dash bonds). All H-atoms except for water, are omitted for clarity.

Table S1: Bonds lengths in [Å] and angles of all crystal structures obtained.

Length [Å]	**LCuMg (1)**	**LCuCa (2)**	**LCuSr (3)**	**LCuBa (4)**		**LNiMg (5)**	**LNiCa (6)**	**LNiSr (7)**	**LNiBa (8)**	
O2 – M_1	1.877(5)	1.884(3)	1.890(7)	1.904(5)		1.832(4)	1.845(2)	1.857(3)	1.800(2)	
O6 – M_1					1.898(4)					1.860(2)
O3 – M_1	1.873(6)	1.902(2)	1.893(5)	1.898(4)		1.827(3)	1.847(2)	1.859(3)	1.860(2)	
O7 – M_1					1.896(5)					1.850(2)
N1 – M_1	1.911(7)	1.931(4)	1.910(9)	1.911(6)		1.830(4)	1.843(3)	1.844(4)	1.880(2)	
N3 – M_1					1.937(6)					1.820(2)
N2 – M_1	1.907(6)	1.918(4)	1.918(8)	1.931(6)		1.822(5)	1.840(2)	1.841(4)	1.870(3)	
N4 – M_1					1.918(7)					1.810(2)
O1 – M_2	2.449(5)	2.566(3)	2.691(6)	2.952(4)		2.463(4)	2.562(2)	2.634(3)	2.990(2)	
O5 – M_2					3.074(5)					2.990(2)
O2 – M_2	2.065(7)	2.378(3)	2.531(7)	2.792(5)		2.065(4)	2.369(2)	2.549(3)	2.800(2)	
O6 – M_2					2.830(5)					2.840(2)
O3 – M_2	2.060(6)	2.372(3)	2.538(5)	2.781(5)		2.069(4)	2.360(2)	2.542(3)	2.810(2)	
O7 – M_2					2.799(5)					2.910(2)
O4 – M_2	2.509(6)	2.614(3)	2.675(6)	3.068(4)		2.446(4)	2.556(2)	2.639(3)	2.930(2)	
O8 – M_2					2.951(4)					2.990(2)
O5 – M_2	2.137(8)	2.437(4)	2.635(9)			2.166(5)		2.691(3)		
O6 – M_2	2.169(7)	2.681(4)	2.682(9)					2.723(4)		
O7 – M_2		2.462(2)								
O8 – M_2	2.002(7)	2.532(3)				1.987(4)	2.401(2)	2.672(4)		
O9 – M_2			2.720(1)	2.965(4)						2.690(2)
O10 – M_2		2.455(4)		2.941(7)				2.653(3)		
O11 – M_2			2.570(7)				2.377(2)	2.578(4)		
O12 – M_2				3.059(7)						2.900(3)
O13 – M_2				2.893(8)						2.930(3)
M_1 – M_2		3.350(1)	3.567(1)	3.738(9)	3.764(1)	3.088(2)	3.393(7)	3.590(6)	3.751(4)	3.796(4)

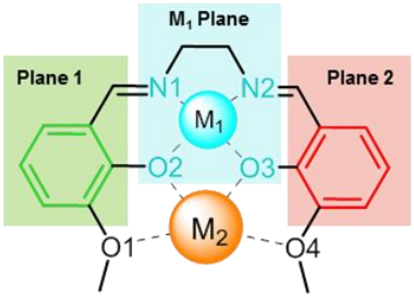

Compounds No.	Ionic radii M_2 (Coord. No.)	Plane 1/ Plane 2	Plane 1/ Cu Plane	Plane 2/ Cu Plane	Cu Plane/ M_2	N_2O_2 Plane-Cu	Cu–M_2	M_2–M_2
1	72 pm (4)	4.85°	7.92°	7.92°	0.008 Å	0.007 Å	3.103(4) Å	-
2	112 pm (8)	16.43°	10.91°	27.13°	0.273 Å	0.078 Å	3.350(1) Å	6.465(1) Å
3	125 pm (8)	3.11°	5.61°	3.11°	0.161 Å	0.027 Å	3.567(1) Å	-
4	160 pm (12)	11.59° and 3.77° 8.62° and 12.98°	3.31° and 5.93° 2.51° and 9.59°	9.28° and 5.15° 6.57°and 4.76°	1.188 and 1.182 Å 1.208 and 1.039 Å	0.017 and 0.000 Å 0.016 and 0.005 Å	3.738(9) and 3.764(1) Å 3.751(8) and 3.752(8) Å	-

Compounds No.	Ionic radii M_2 (Coord. No.)	Plane 1/ Plane 2	Plane 1/ Ni Plane	Plane 2/ Ni Plane	Ni Plane/ M_2	N_2O_2 Plane-Ni	Ni–M_2
5	72 pm (4)	2.72°	5.50°	3.97°	0.232 Å	0.003 Å	3.088(4) Å
6	112 pm (8)	3.50°	10.53°	8.01°	0.218 Å	0.010 Å	3.393(9) Å
7	125 pm (8)	2.03°	8.16°	6.16°	0.150 Å	0.009 Å	3.391(6) Å
8	160 pm (12)	2.42° and 12.06° 6.32° and 10.52°	8.23° and 8.69° 4.29° and 6.89°	8.27° and 4.09° 3.93° and 3.63°	1.225 and 1.218 Å 1.233 Å and 1.096 Å	0.033 and 0.004 Å 0.027 and 0.009 Å	3.798(4) and 3.742(4) Å 3.796(4) and 3.750(4) Å